© 2019. Published by The Company of Biologists Ltd | Development (2019) 146, dev171181. doi:10.1242/dev.171181

RESEARCH ARTICLE

Maize *YABBY* genes *drooping leaf1* and *drooping leaf2* regulate floret development and floral meristem determinacy

Josh Strable[1,2,*,‡] and Erik Vollbrecht[1,2,‡]

ABSTRACT

Floral morphology is shaped by factors that modulate floral meristem activity and size, and the identity, number and arrangement of the lateral organs they form. We report here that the maize *CRABS CLAW* co-orthologs *drooping leaf1* (*drl1*) and *drl2* are required for development of ear and tassel florets. Pistillate florets of *drl1* ears are sterile with unfused carpels that fail to enclose an expanded nucellus-like structure. Staminate florets of *drl1* tassels have extra stamens and fertile anthers. Natural variation and transposon alleles of *drl2* enhance *drl1* mutant phenotypes by reducing floral meristem (FM) determinacy. The *drl* paralogs are co-expressed in lateral floral primordia, but not within the FM. *drl* expression together with the more indeterminate mutant FMs suggest that the *drl* genes regulate FM activity and impose meristem determinacy non-cell-autonomously from differentiating cells in lateral floral organs. We used gene regulatory network inference, genetic interaction and expression analyses to suggest that DRL1 and ZAG1 target each other and a common set of downstream genes that function during floret development, thus defining a regulatory module that fine-tunes floret patterning and FM determinacy.

KEY WORDS: Maize, Meristem determinacy, Floret development, Non-cell-autonomous action

INTRODUCTION

A major goal in plant biology is to understand the factors that regulate meristem activity. Meristems, which are active, pluripotent stem cell tissues, produce all postembryonic organs of flowering plants (Greb and Lohmann, 2016). Meristem determinacy (degree of meristem activity) is a crucial factor that shapes vegetative, inflorescence and floral architectures. Vegetative and inflorescence meristems are indeterminate, producing an unspecified number of lateral primordia. Floral meristems (FMs) are generally determinate, initiating a set number of floral whorls and organs before undergoing terminal differentiation. Commonly, eudicot flowers are composed of four whorls of floral organs (outermost to innermost: sepal, petal, stamen and carpel). Similarly, in the monocots grass florets (flowers), including those in maize (*Zea mays*), are arranged in whorls of floral organs, some of which have grass-specific names (outermost to innermost: lemma, palea, stamen and carpel). As each grain is the product of one floret, regulation of FM activity is a key agronomic trait.

[1]Department of Genetics, Development and Cell Biology, Iowa State University, Ames, IA 50011, USA. [2]Interdepartmental Plant Biology, Iowa State University, Ames, IA 50011, USA.
*Present address: School of Integrative Plant Science, Section of Plant Biology, Cornell University, Ithaca, NY 14853, USA.

‡Authors for correspondence (jjs369@cornell.edu; vollbrec@iastate.edu)

J.S., 0000-0002-0260-8285; E.V., 0000-0003-4919-1365

Received 24 August 2018; Accepted 18 February 2019

FMs pattern flowers through the combinatorial activity of three classes of gene functions that dictate organ identity and FM determinacy (Coen and Meyerowitz, 1991; Pelaz et al., 2000). In *Arabidopsis thaliana*, carpels are specified by the MADS-box transcription factor AGAMOUS (AG) (Yanofsky et al., 1990). AG is expressed in the FM and controls FM determinacy by repressing expression of the stem cell regulator *WUSCHEL* (Lenhard et al., 2001; Lohmann et al., 2001). In the cereals, AG orthologs have expanded and undergone subfunctionalization during grass evolution, leading to redundancy in the regulation of FM determinacy (Mena et al., 1996; Yamaguchi et al., 2006; Dreni et al., 2011). The maize *AG* ortholog *zea agamous1* (*zag1*) imposes FM determinacy with less obvious roles in regulating floret organ identity as supernumerary carpels develop in pistillate florets of *zag1* mutants (Mena et al., 1996). ZAG1 interacts physically with the AG-LIKE6 (AGL6) subfamily member bearded ear (BDE; also known as ZAG3), and *zag1; bde* double mutants reveal a synergistic interaction in regulating FM determinacy (Thompson et al., 2009). Pistillate and staminate FMs are more indeterminant in the maize *indeterminate floral apex1* (*ifa1*) mutant, and *ifa1* interacts synergistically with *zag1* to regulate FM determinacy (Laudencia-Chingcuanco and Hake, 2002). In the bisexual florets of rice (*Oryza sativa*), *AG* orthologs *OsMADS3* and *OsMADS58* regulate floret organ identity and FM determinacy, respectively (Yamaguchi et al., 2006; Dreni et al., 2011).

The *Arabidopsis YABBY* family member *CRABS CLAW* (*CRC*) is required for proper growth of the gynoecium (Alvarez and Smyth, 1999). Loss-of-function mutations in *CRC* consistently reduce stylar growth and result in incomplete medial fusion of carpels. *crc* mutants occasionally produce three carpels compared with two in wild type, suggesting that *CRC* is necessary to promote FM determinacy (Alvarez and Smyth, 1999; Bowman and Smyth, 1999). Expression of *CRC* is restricted laterally to developing carpels and nectaries (Bowman and Smyth, 1999). The rice *CRC* ortholog *DROOPING LEAF* (*DL*) is required for carpel identity, as carpels undergo homeotic transformation to stamens in strong loss-of-function alleles of *dl* mutants (Yamaguchi et al., 2004). Transformed stamens are variable in number, indicating that *DL* also regulates FM determinacy. *DL* is expressed in carpel primordia of rice florets (Yamaguchi et al., 2004). Genetic analysis indicates that *DL* and the rice *AGL6* subfamily member *MOSAIC FLORAL ORGAN 1*/*OsMADS6* redundantly regulate FM determinacy (Li et al., 2011).

Here, we report that the maize *CRC* co-orthologs *drooping leaf1* (*drl1*) and *drl2* are required for the development of dimorphic, unisexual ear and tassel florets. *drl1* floret phenotypes and FM indeterminacy are enhanced by natural variant and transposon alleles of *drl2*. The *drl* paralogs are co-expressed in lateral organ primordia initiated by the FM, but not within the FM. Gene regulatory network (GRN) inference, genetic interaction and expression analyses suggest that DRL1 and ZAG1 target each other

Development (2019) 146, dev171181. doi:10.1242/dev.171181

and a common set of downstream genes that function during floret development. Our results demonstrate that the *drl* genes are required for floret patterning, to impose meristem determinacy via some non-cell-autonomous mechanism, and, together with *zag1*, define a regulatory module that provides crucial control of floret patterning and FM determinacy in the development of grain-producing structures.

RESULTS

drl1 and *drl2* regulate floret development

Maize staminate and pistillate florets are produced on the tassel and ear, respectively (Kiesselbach, 1949). During tassel and ear development, branching events from multiple meristem types (Irish, 1997) ultimately give rise to floret whorls housed in grass-specific spikelets (Clifford, 1987). The indeterminate inflorescence meristem (IM) of the tassel and ear initiates determinate spikelet pair meristems (SPMs); additionally, in the tassel the IM initiates indeterminate branch meristems (BMs). Each SPM produces a pair of determinate spikelet meristems (SMs), each of which gives rise to two glumes. Afterwards, each SM initiates a lower floral meristem (LFM) and then converts identity to an upper floral meristem (UFM). Each determinate LFM and UFM gives rise to a lemma, a palea, two lateral-abaxial lodicules, three stamens and three carpels (Cheng et al., 1983). Two lateral-adaxial stamens are spaced widely relative to the medial-abaxial stamen (Irish et al., 2003). Three connately fused carpels form the single pistil; however, only the two lateral-abaxial carpels (indeterminate carpels, C_i) form an elongated silk, whereas growth of the medial-adaxial carpel (determinate carpel, C_d) is limited in growth to envelop the single ovule (Randolph, 1926; Bonnett, 1953). The ovule consists of a mostly enclosing inner and a partially enclosing outer integument plus nucellar tissue that contains the embryo sac, and fills the locule formed by the three fused carpels (Kiesselbach, 1949). After organ initiation, sex determination in the tassel and ear culminates in abortion of the carpel whorl in staminate florets and arrest of stamen primordia in pistillate florets, respectively (Cheng et al., 1983) (Fig. 1A,B).

Likely null mutations of *drl1* displayed aberrant pistillate and staminate floret morphologies. Macroscopically, *drl1* mutant ears were sterile, with underdeveloped silks consisting of reduced, unfused carpel walls that failed to enclose an expanded nucellus-like structure (Fig. 1C,D). *drl1* pistillate phenotypes were reminiscent of the floret phenotypes described for the *ifa1* mutant (Laudencia-Chingcuanco and Hake, 2002). We found *drl1* and *ifa1* to be allelic through genetic noncomplementation of mutant alleles (Fig. S1) and by sequencing the *drl1* locus in *ifa1* mutant plants (Strable et al., 2017). *drl1* and its paralogous genetic enhancer locus, *drl2*, encode *CRC* co-orthologs in the YABBY family of transcriptional regulators (Strable et al., 2017). Genetic combinations between *drl1* alleles and the loss of- or low-function *drl2-Mo17* natural variant allele (hereafter referred to as *drl2-M*) or the strong *drl2-DsD08* transposon allele (Strable et al., 2017) enhanced all aspects of the *drl1* floret phenotype, such that florets from double mutants displayed multiple, expanded nucellus-like structures that appeared to originate from sustained FM activity in the upper floret (UF) (Fig. 1C,D; Fig. S2). The synergistic genetic interactions between *drl1* and *drl2* mutant and natural variant alleles in florets were dose sensitive, consistent with dosage effects observed for vegetative traits (Strable et al., 2017). In an F_2 population with varied dosage of *drl2-M*, florets of *drl1-R; drl2-M/+* plants were intermediate in severity between *drl1-R* homozygotes and *drl1-R; drl2-M* double homozygotes (Fig. 1C). Collectively, these observations suggest that the *drl* loci regulate pistillate floret development in a dose-dependent manner.

In the *drl1* mutant tassel, we observed an ectopic stamen periodically in the UF of sessile [3.14±0.06 (mean±s.e.m.)] and pedicellate (3.05±0.04) spikelets, compared with three stamens in normal spikelets (Fig. 1E-G). Histological examination of mature *drl1* mutant spikelets revealed that the infrequent extra stamen originated internal to the normally placed and numbered lemma and palea in the outer whorl (Fig. 1F). FM indeterminacy was enhanced in *drl1; drl2* double mutants, in which stamen number was increased in both the UF and lower floret (LF) of sessile [4.49±0.09 (P=1.0×10^{-19}) and 3.41±0.08 (P=4.6×10^{-6}), respectively] and pedicellate [3.92±0.11 (P=3.0×10^{-10}) and 3.19±0.08 (P=0.015), respectively] spikelets (Fig. 1E-G). Such differences were significant between stamen number in the UF and LF within sessile and within pedicellate spikelets (P<10^{-6}), and for UFs, between sessile and pedicellate spikelets (P<10^{-3}) (Fig. 1G). These data suggest that the *drl* genes participate differentially in determinacy pathways of upper and lower staminate FMs. An alternative explanation is that the *drl* genes function equally in UFM and LFM determinacy pathways, but that LFM determinacy is more hardwired relative to the UFM, which is therefore perhaps more sensitized to loss of *drl* gene function. Finally, the observations also suggest that ectopic stamens originate from sustained activity of the mutant FM.

Some floret phenotypes were specific to *drl1; drl2* double mutants. We observed an ectopic primordium with lodicule-like cellular morphology and vascularization occasionally in the position of a presumptive, suppressed adaxial-medial lodicule in the UF (Fig. 1F, right panel, arrowhead), indicating a possible role for *drl* gene products in imposing zygomorphy (Irish et al., 2003; Bartlett et al., 2015). We also observed macrohair-like structures along the apical ridge of *drl1-R; drl2-M* supernumerary anthers (Fig. S3). Macrohair production is generally limited to the adaxial epidermis of the adult leaf blade and is frequently used as a morphological marker for leaf polarity (Juarez et al., 2004). Though these ectopic structures were infrequent, they lacked the multicellular bases of leaf blade macrohairs (Becraft and Freeling, 1994) and were consistently associated with supernumerary anthers with altered morphology. Such amorphic anthers had aberrant theca that lacked pollen sacs and were often fused to morphologically normal anthers. These data suggest that the *drl* genes are necessary for complete suppression of macrohair formation on reproductive floral organs, similar to *AG* and *SHATTERPROOF1/2* in suppressing trichome initiation on floral organs in *Arabidopsis* (Ó'Maoiléidigh et al., 2018). Alternatively, the ectopic structures may be a mosaic of anther and leaf identities due to a partial loss of stamen identity in *drl1; drl2* double mutants.

drl1 and *drl2* impose floral meristem determinacy

We tracked the developmental basis of *drl1* and *drl1; drl2* mutant phenotypes in mid- and later-staged pistillate florets with scanning electron microscopy (SEM). Prior to sex determination, the inner whorl of normal UFs consisted of a medial-adaxial C_d primordium (determinate carpel) and two lateral-adaxial C_i primordia (indeterminate carpels), all of which were connately fused (Fig. 2A). This gynoecial whorl was flanked by a whorl of three pre-degenerate stamen primordia. The LF lagged in development, with an FM and recently initiated stamen primordia (Fig. 2A). In mid-staged UFs of *drl1* mutants, the medial-adaxial C_d initiated with extreme delay or, often, not at all (Fig. 2B,C). Carpel walls did not fuse entirely in *drl1* mutants, and development of integument tissues appeared to be compromised (Fig. 2B,C), resulting in the eventual single protruding nucellus-like structure observed in mature *drl1* mutant florets (Fig. 1D). *drl1* mutant UFs had extra whorls of lateral

Development (2019) 146, dev171181. doi:10.1242/dev.171181

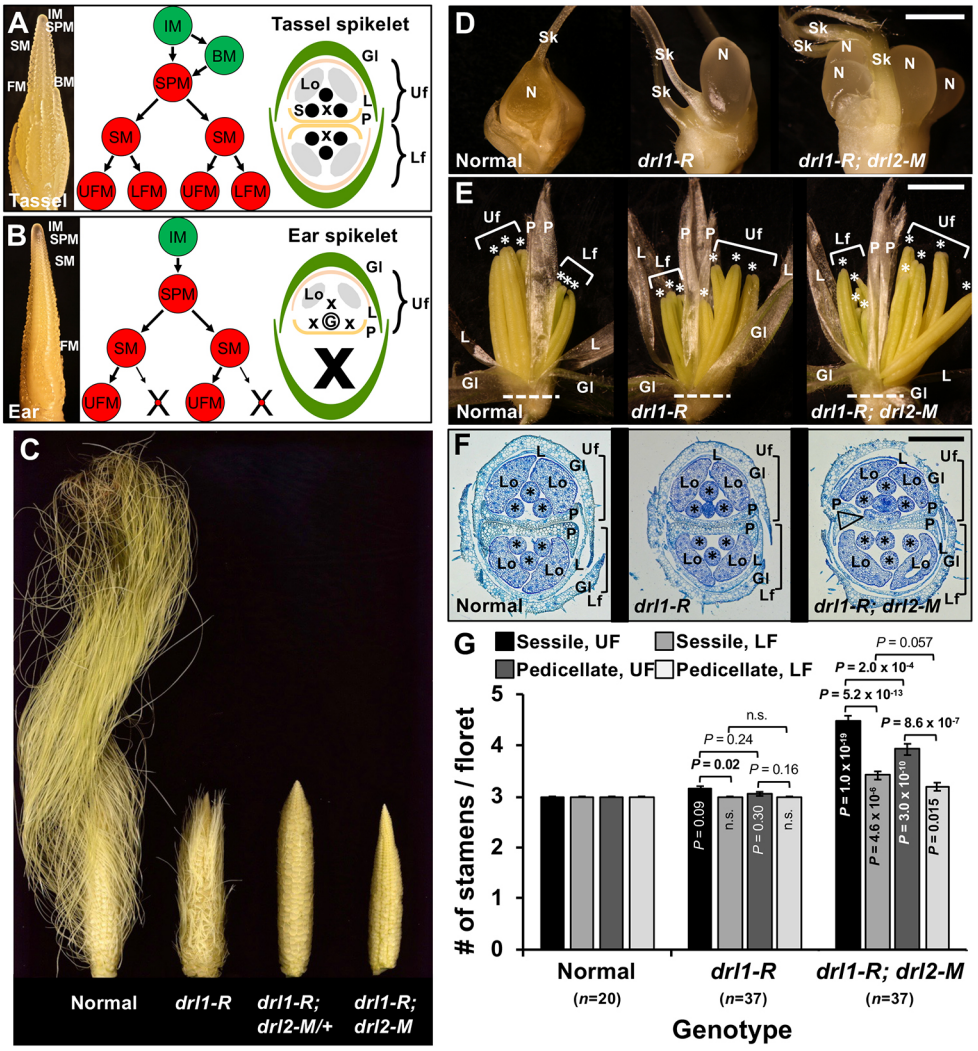

Fig. 1. Floral architecture in *drl1* single and *drl1; drl2* double mutants. (A) Development of the maize tassel and staminate florets. Left: developing tassel (6 mm). Middle: the IM gives rise to BMs and SPMs, which in turn produce SMs which each give rise to one UFM and one LFM. Right: a tassel spikelet consists of outer and inner glumes that house the UF and LF, each of which comprises a lemma and palea, two lodicules and three stamens. (B) Development of the maize ear and pistillate florets. Left: developing ear (6 mm). Middle: the IM gives rise to SPMs that produce SMs, which each give rise to one UFM and one LFM; the LFM aborts early. Right: an ear spikelet consists of outer and inner glumes that house the UF, which comprises a lemma and palea, two reduced lodicules and a gynoecium. (C) Mature ears from an F_2 population showing dosage effects of the *drl* loci. Left to right: normal, *drl1-R*, *drl1-R; drl2-M*/+ and *drl1-R; drl2-M*. (D) Dissected pistillate spikelet of normal (left, bisected), *drl1-R* (middle, intact) and *drl1-R; drl2-M* (right, intact). (E) Dissected staminate spikelet of normal (left), *drl1-R* (middle) and *drl1-R; drl2-M* (right). (F) Transverse sections of staminate spikelets stained with Toluidine Blue O taken at the plane of the dashed line in E; normal (left), *drl1-R* (middle) and *drl1-R; drl2-M* (right). (G) Quantification of stamens in normal, *drl1-R* and *drl1-R; drl2-M* florets. Mean±s.e.m., *P*-values based on two-tailed Student's *t*-tests; *n*, sample size. G, gynoecium; Gl, glume; L, lemma; Lf, lower floret; Lo, lodicule; N, nucellus-like structure; P, palea; S, stamen; Sk, silk; Uf, upper floret; X, aborted organ. Asterisks mark mature anthers. Arrowhead (F) marks ectopic organ. Scale bars: 2 mm (D,E); 200 µm (F).

C_i (Fig. 2C); however, shifts in phyllotaxis between each extra whorl complicated assigning ab- or adaxial orientation relative to the palea axil. The medial-adaxial C_d was similarly greatly reduced or suppressed in mid-staged UFs of *drl1; drl2* double mutants, yet the double mutants displayed multiple whorls of lateral C_i indicating prolonged FM activity (Fig. 2D-F). Additionally in the axil of each C_i whorl of *drl1; drl2* double mutants, we frequently observed an ectopic structure that we interpreted to be a lodicule-like and/or anther-like primordium based on position and morphology (Fig. 2D-F, asterisks).

In normal later-staged UFs, lateral-adaxial C_i primordia appeared paired and elongate, whereas the reduced medial-adaxial C_d was a ridge of cells just prior to enveloping of the ovule (Fig. 2G). Multiple whorls of paired lateral-adaxial C_i primordia were obvious in similarly staged *drl1* mutant UFs (Fig. 2H), whereas lateral-adaxial C_i primordia observed in later-staged UFs of *drl1; drl2* double mutants indicated the presence of an extra, intra-whorl fused or partially fused C_i primordium (Fig. 2I). Additionally, we often detected involution of the palea, or, alternatively, partial fusion of paleas, along the medial axis in *drl1; drl2* double mutant florets (Fig. 2E,I, arrowheads), which may indicate crowding within the inner whorl of the floret or ectopic palea that initiate within their normal whorl. Taken together, these observations indicate that the *drl* genes are required for proper patterning of pistillate florets, including C_d elaboration or initiation, and to impose FM determinacy.

drl genes are expressed dynamically throughout inflorescence development and solely in lateral primordia

To examine the temporal and spatial patterns of *drl* transcript accumulation during inflorescence and floret development, we

Development (2019) 146, dev171181. doi:10.1242/dev.171181

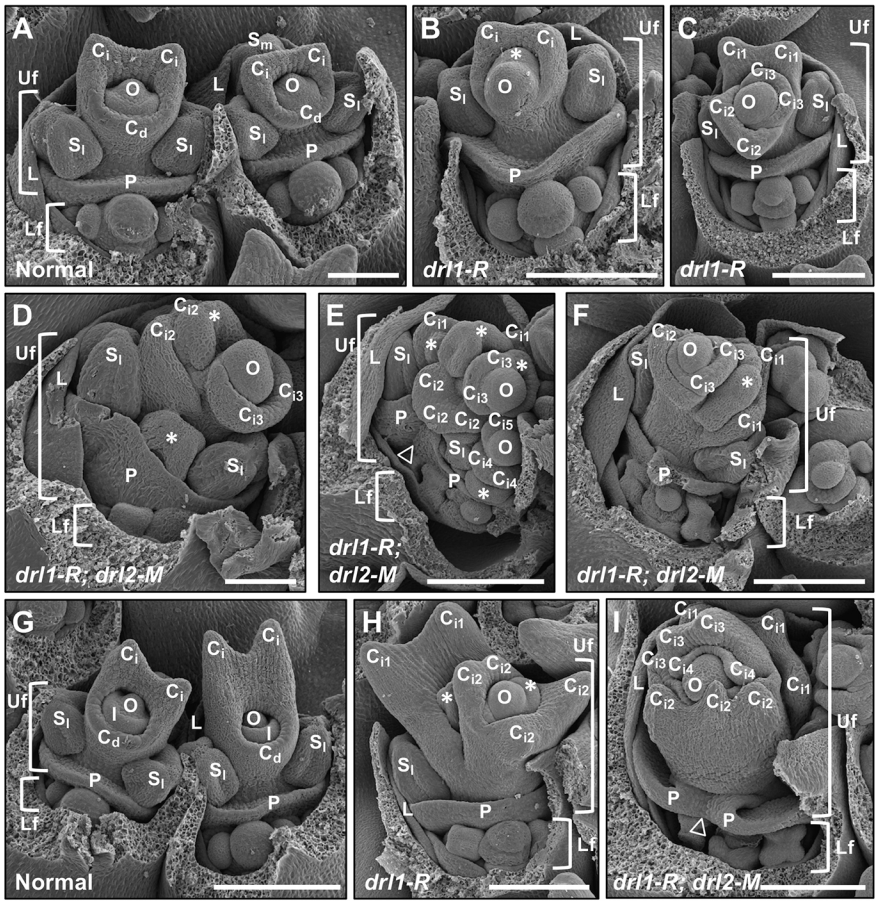

Fig. 2. Development of pistillate florets in *drl1* single and *drl1; drl2* double mutants. (A-F) SEM of mid-staged pistillate florets from normal (A), *drl1-R* (B,C) and *drl1-R; drl2-M* (D-F) developing ears. (G-I) SEM of late-staged pistillate florets from normal (G), *drl1-R* (H) and *drl1-R; drl2-M* (I) developing ears. Glumes were removed manually to expose the upper and lower florets. C_d, determinate carpel primordium; C_i, indeterminate carpel primordium (whorl number is subscripted); I, integument; L, lemma primordium; Lf, lower floret; O, ovule primordium; P, palea primordium; S_l, lateral stamen primordium; S_m, medial stamen primordium; Uf, upper floret. Asterisks (B,D,E,H) mark ectopic primordia. Arrowhead (I) points to palea involution. Scale bars: 100 µm (A,D); 200 µm (B,C,E-I).

performed RNA *in situ* hybridization. In median longitudinal sections of the developing ear, *drl1* transcripts were detected in the IM periphery, which spatially corresponds to cryptic bract anlagen (Whipple et al., 2010) (Fig. S4A). *drl1* transcripts continued to accumulate in outer glume primordia (Fig. 3A), but not in the SM, as marked by accumulation of *knotted1* (*kn1*) transcripts (Jackson et al., 1994) (Fig. 3B). The accumulation pattern of *drl1* transcripts persisted in lateral organs of later-staged SMs where they were detected in lemma and palea primordia (Fig. 3C,D, Fig. S4B), expression patterns that were also observed for *drl2* (Fig. S4C). In more advanced pistillate florets, *drl1* transcripts accumulated in carpel primordia that had initiated in the UF and LF, but not in the central presumptive ovule primordium of either floret (Fig. 3E,F). In developing staminate florets, *drl1* transcripts accumulated similarly in lateral primordia that were initiated by the FM, but not within the FM (Fig. 3G,H). *drl* expression dynamics across developing inflorescences were supported using publicly available transcriptomic data (Fig. S4E; www.maizeinflorescence.org). To summarize, the *drl* genes were expressed in cryptic bracts, in lateral organ primordia initiated by the SM (glumes), and in primordia of outer (lemma and palea) and inner (carpels) whorl organs initiated by the FM. *drl* expression in carpel primordia correlated with the organs for which development was altered in *drl1* and *drl1; drl2* mutant florets. However, the indeterminate FMs observed in *drl* mutant florets are best explained by mis-regulation of FM activity, yet *drl* expression was limited to organs derived from the meristems and was excluded from the meristem. These points strongly suggest that *drl* regulates meristem activity via a non-cell-autonomous mechanism. Consistent with this hypothesis, *drl1* and *drl1; drl2* mutants also display a dose-dependent reduction in vegetative shoot apical meristem (SAM) size even though the *drl* genes are expressed in leaf primordia and not in the SAM proper (Strable et al., 2017).

To interpret the indeterminant *drl* mutant pistillate florets further, we examined the expression patterns of the *FILAMENTOUS FLOWER* homolog *zea zyb15* (also known as *yabby15* or *yabby8*) (Strable et al., 2017) and *kn1* (Jackson et al., 1994) in the *drl1-R; drl2-M/+* background. In the inflorescence, *zyb15* is expressed in cryptic bract (Whipple et al., 2010) and outer whorl primordia of florets (Gallavotti et al., 2011). We observed *zyb15* transcript accumulation in glume, lemma, palea and carpel primordia, but not in the FM or in stamen primordia, for both normal and *drl1-R; drl2-M/+* developing pistillate UF and LF (Fig. 3I-N). Interestingly, *zyb15* transcript accumulation persisted longer in glume primordia compared with *drl1* accumulation (Fig. 3M, compare with 3E). The *kn1* gene is expressed in meristematic cells and is downregulated in cells recruited to form a lateral domain on the flank of the meristem and in lateral organ primordia (Jackson et al., 1994). We observed that *kn1* transcripts were absent from normal later-staged pistillate UFs that had undergone terminal differentiation to an ovule primodium, whereas in similarly staged *drl1* mutant UFs, *kn1* transcript accumulation persisted throughout the gynoecial axis, demonstrating that *drl1; drl2* FMs are more indeterminate (Fig. 3O).

GRN inference predicts a DRL1-ZAG1 regulatory module in developing florets

In maize, FM determinacy is regulated redundantly by *zag1* and *bde* genes, both of which are expressed dynamically throughout floret development, including in the FM, and whose encoded proteins physically interact (Schmidt et al., 1993; Mena et al., 1996;

Development (2019) 146, dev171181. doi:10.1242/dev.171181

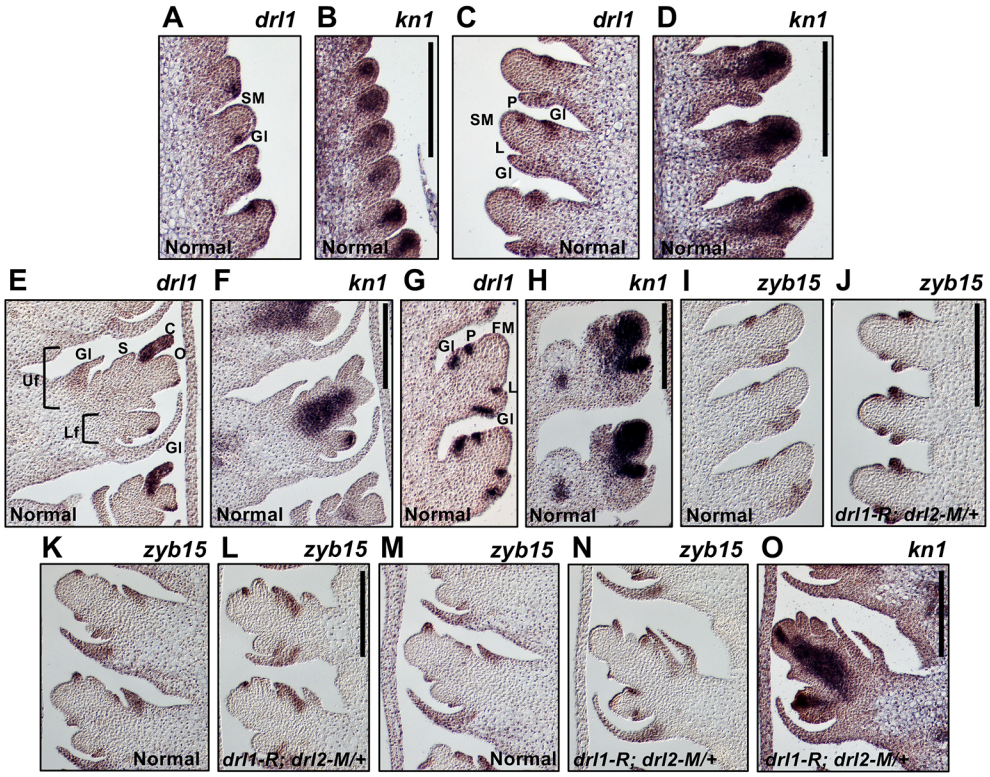

Fig. 3. RNA *in situ* hybridization of normal pistillate and staminate florets and *drl1-R; drl2-M*/+ mutant pistillate florets. (A-O) Longitudinal sections through developing normal ears (A-F,I,K, M), normal tassels (G,H) or *drl1-R; drl2-M*/+ ears (J,L,N,O) hybridized with antisense RNA probes to *drl1* (A,C,E,G), *kn1* (B,D,F,H,O) or *zyb15* (I-N). C, carpel primordium; Gl, glume primordium; L, lemma primordium; Lf, lower floret; O, ovule primordium; P, palea primordium; S, stamen primordium; Uf, upper floret. Scale bars: 200 µm.

Thompson et al., 2009). Additionally, the *ifa1* allele imposes FM determinacy redundantly with *zag1* (Laudencia-Chingcuanco and Hake, 2002). Similarly, we observed extreme loss of determinacy in pistillate florets of *zag1-mum1; drl1-R; drl2-M* triple mutants, in which floret axes displayed iterative secondary and tertiary branch-like lateral growth from the axils of ectopic palea or bracts (Fig. 4A-E).

To gain insight into a potential regulatory module and shared targets for DRL1 and ZAG1, we mined an integrated atlas of gene expression, protein abundance, and regulatory networks generated from multiple tissues, including ear florets, across maize development (Walley et al., 2016). From this atlas, Walley and co-workers demonstrated that integrating transcriptome, proteome and phosphoproteome datasets into unified GRNs significantly improved the predicative power of the GRN. *drl1*, *drl2* and *zag1* mRNAs and their encoded non-modified proteins and phosphoproteins accumulated differentially throughout pistillate floret development (Fig. 4G). When classified as regulators in the integrative transcriptome, proteome and phosphoproteome GRN, DRL1 and ZAG1 transcription factors shared 51.4% of their target genes (Fig. 4H), implying that DRL1 and ZAG1 co-regulate many genes to control floret development. Among the high-confidence edge scores, DRL1 is predicted to target seven of the 13 YABBY family members, including itself and *drl2* (Fig. 4I, column 7), indicating potential auto- and cross-regulation activities at the *drl* loci, a hypothesis that is supported genetically by dosage-related phenotypes in *drl1* and *drl2* mutant ears (Fig. 1C). The seven YABBY target genes are expressed throughout inflorescence development, and a majority of them show peak expression levels in late-staged ears and tassels, which parallels floret development (Fig. 4I, ear and tassel columns). Furthermore, *drl1*, *drl2* and *yab5* are shared predicted high-confidence target genes with ZAG1 (Fig. 4I). We next looked at high-confidence MADS box target genes predicted to be shared between DRL1 and ZAG1 regulators and found 26 genes that are potentially co-regulated and are co-expressed during inflorescence development (Fig. 4I). Among the co-regulated target genes are *zag1* and *bde*, which have been shown previously to have roles in floral development and meristem determinacy (Mena et al., 1996; Thompson et al., 2009). The extreme loss of determinacy in *zag1-mum1; drl1-R; drl2-M* triple mutant pistillate florets (Fig. 4A-E) and ectopic *zag1* transcript accumulation in late-staged *drl1-R; drl2-M* double mutant ears (Fig. 4J) supports a putative complex relationship between DRL1-ZAG1 regulators and their *drl1*, *drl2* and *zag1* targets. DRL1 and ZAG1 are predicted to target *silky1* (*si1*) (Fig. 4I), the maize *APETALA3/DEFICIENS* ortholog, which is required for lodicule and stamen identity, and is expressed in developing lodicule and stamen primordia of staminate and pistillate florets (Ambrose et al., 2000; Chuck et al., 2008; Bartlett et al., 2015). We found *si1* to be mis-expressed at earlier developmental stages in *drl1-R; drl2-M* double mutant ears compared with its late-stage expression in ears from normal siblings (Fig. 4J). We explored this result by RNA *in situ* hybridization in *drl1-R; drl2-M*/+ ears and found *si1* transcript accumulation marked ectopic primordia in the UF and was strongly expressed throughout the LF (Fig. S5). By comparison, in normal pistillate UFs and in the LFs *si1* expression was restricted to degenerating stamen primordia and lodicules. The mis-expression of *si1*, together with the appearance of ectopic lodicule-like and/or anther-like structures in axil of each Ci whorl of *drl1; drl2* double mutants (Fig. 2), suggests that the *drl* genes are necessary to promote and/or maintain boundary identity between their expressed whorl 4 and adjacent floret whorls by suppressing *si1* expression.

We uncovered floral-expressed genes that had been characterized previously but not described as putative targets of DRL1 and ZAG1. These candidate genes include the squamosa promoter-binding transcription factor-encoding *teosinte glume architecture1* (Wang et al., 2005) and the *ASYMMETRIC LEAVES 2* (*AS2*) homologs *indeterminate gametophyte1* (*ig1*) and *ig1-as2 like1* (Evans, 2007).

Development (2019) 146, dev171181. doi:10.1242/dev.171181

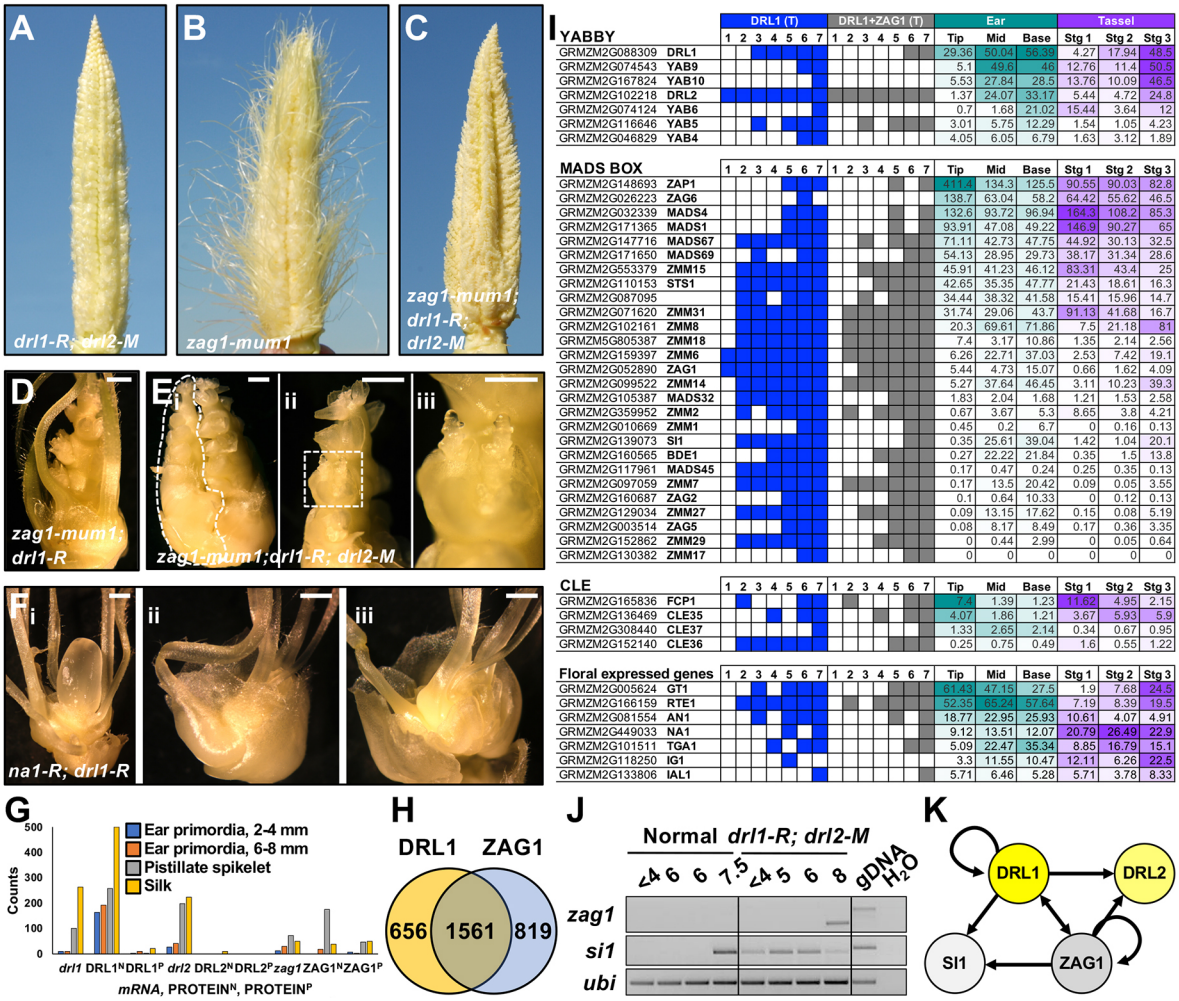

Fig. 4. GRN inference identifies causal genetic relationships between *drl* and candidate floret and meristem genes. (A-E) Genetic interaction analysis between *drl1-R; drl2-M; zag1-mum1* higher-order mutants in field-grown mature ears (A-C) and dissected pistillate florets (D,Ei-iii; floret outlined in E_i is shown in Eii; boxed region in Eii is enlarged in Eii). (Fi-iii) Genetic interaction analysis between *drl1-R; na1-R* double mutants in field-grown dissected pistillate florets; double mutant phenotypes ranged from mild (i), a single large nucellus surrounded by ectopic pistils, to enhanced with reduced florets with many ectopic pistils (ii, iii). (G) mRNA (in normalized FPKM), non-modified protein (in normalized dNSAF) and phosphoprotein (in normalized spectral counts) levels from developing and mature floret tissue (Walley et al., 2016). (H) Venn diagram of GRN inference from integrating mRNA, non-modified protein, and phosphoprotein datasets (Walley et al., 2016) for DRL1 and ZAG1 regulators. (I) High-confidence edge score candidate target genes identified by GRN inference for DRL1 (blue) or DRL1-ZAG1 (gray) regulators. GRNs for mRNA (1); non-modified protein (2); phosphoprotein (3); mRNA+non-modified protein (4); mRNA+phosphoprotein (5); non-modified protein+phosphoprotein (6); mRNA+non-modified protein+phosphoprotein (7) (Walley et al., 2016). Right-hand side shows heat map of RNAseq data (in RPKM; www.maizeinflorescence.org) scaled by gene family for B73 ear tip (1 mm section from the tip of a 10 mm ear, enriched for IM and SPMs), middle (2 mm section 2 mm from the tip of a 10 mm ear, enriched for SMs) and base (2 mm section 6 mm from the tip of a 10 mm ear, enriched for FMs), and B73 tassels stage 1 (1-2 mm), stage 2 (3-4 mm) and stage 3 (5-7 mm). (J) Reverse transcription followed by semi-quantitative PCR of *zag1*, *si1* and *ubiquitin* (*ubi*) gene expression in field-grown ears harvested at the developmental stages (ear lengths in mm) labeled above each lane. Data are for 33 PCR cycles; genomic DNA positive control, water negative control. (K) Model proposing a relationship among DRL1, ZAG1, DRL2 and SI1 during floret development. Scale bars: 1 mm.

Other candidate DRL1 and ZAG1 target genes are required for the development of dimorphic, unisexual ear and tassel florets, such as *anther ear1*, which encodes a gibberellin biosynthetic enzyme necessary to promote stamen abortion in pistillate florets (Bensen et al., 1995), *grassy tillers1*, which encodes a homeodomain leucine zipper transcription factor required to repress carpel growth in staminate florets (Whipple et al., 2011), and *nana plant1* (*na1*), which encodes a brassinosteriod biosynthetic enzyme that represses carpel growth in the center whorl of staminate florets (Hartwig et al., 2011). We tested the relationship between *na1* and *drl* genes through genetic interaction analysis. Pistillate florets of *na1-R; drl1-R* double mutant ears ranged from a single large nucellus subtended by ectopic pistils to reduced florets with many ectopic pistils (Fig. 4F). We observed normal, unisexual staminate florets in *na1-R* tassels for both greenhouse and field conditions (Fig. S6), suggesting that the tasselseed phenotype is specific to allele, genetic background and/or environmental condition.

DISCUSSION

Genetic, expression and evolutionary analyses indicate that *CRC* and orthologous genes are key regulators of floral development across diverse angiosperms (Alvarez and Smyth, 1999; Bowman and Smyth, 1999; Eshed et al., 1999; Yamaguchi et al., 2004; Fourquin et al., 2005, 2014; Orashakova et al., 2009; Nakayama et al., 2010; Yamada et al., 2011; Pfannebecker et al., 2017). Our results demonstrate crucial roles for the maize *drl* genes in regulating stem cell homeostasis and patterning of inner-whorl organs in dimorphic, unisexual florets. Unexpected findings of this study were the presence of ectopic

Development (2019) 146, dev171181. doi:10.1242/dev.171181

primordia with lodicule-like cellular morphology, vascularization and medial placement in staminate florets (Fig. 1F), and, in the axils of carpel primordia in pistillate florets, the development of ectopic structures that we interpreted to be lodicule-like or anther-like primordia based on morphology and position (Fig. 2). These observations, together with the mis-expression of *si1* in *drl1; drl2* double mutant ears (Fig. 4J, Fig. S5), strongly hints at a possible antagonistic relationship between *drl* genes and the B-class MADS box gene *si1* that specify lodicule (whorl 3) and stamen (whorl 2) identities (Ambrose et al., 2000; Bartlett et al., 2015). Understanding the genetic relationship between the *drl* genes and B-class genes *si1* (Ambrose et al., 2000) and *sterile tassel silky ear1* (Bartlett et al., 2015) may help clarify mechanisms that underlie their function in floret patterning and potentially in regulating developmental programs that control zygomorphy.

We hypothesize that the *drl* gene products function non-cell-autonomously in or through pathways that signal from lateral primordia, through boundary domains, to regulate developmental programs that impose FM determinacy. Typically, FMs terminate upon correct spatiotemporal initiation of all floral organ primordia. In *Arabidopsis*, cessation of FM activity is concurrent with the expression of *AG*, which integrates stem cell homeostasis with floral patterning pathways; AG directly represses *WUS* expression and subsequently FM activity is lost (Lenhard et al., 2001; Lohmann et al., 2001). AG indirectly represses *WUS* expression by directly activating the expression of *KNUCKLES* (*KNU*), which encodes a C2H2 zinc-finger transcription factor that directly represses *WUS* (Payne et al., 2004; Sun et al., 2009). *KNU* (Sun et al., 2009, 2014) and *CRC* (Gómez-Mena et al., 2005; Ó'Maoiléidigh et al., 2013) are direct targets of AG and function in parallel to regulate FM determinacy (Yamaguchi et al., 2017). *crc; knu* double mutants display a synergistic interaction with a highly indeterminate floral axis (Yamaguchi et al., 2017). Recently, CRC and CRC-AG were shown to impose FM determinacy by controlling auxin homeostatic (Yamaguchi et al., 2017) and biosynthetic (Yamaguchi et al., 2018) pathways, respectively. However, whereas *WUS*, *AG* and *KNU* expression domains overlap spatially and temporally in the FM during floral development (Lenhard et al., 2001; Lohmann et al., 2001; Sun et al., 2014), *CRC* is expressed in adjacent lateral carpel primordia at slightly later developmental stages (Bowman and Smyth, 1999), suggesting additional factors may provide requisite spatiotemporal inputs (Goldshmidt et al., 2008). Unlike in *Arabidopsis*, *WUS* orthologs in maize that specify the floral stem cell niche have not been functionally characterized. In maize, *zag1* regulates FM determinacy with a lesser role in promoting carpel identity; currently, functional analyses have not been reported for the *zea mays mads2* paralog (*zmm2*; Mena et al., 1996). *zag1* and *zmm2* expression domains overlap largely throughout the development of pistillate florets, where they mark the FM, as well as stamen and carpel primordia (Schmidt et al., 1993; Chuck et al., 2008). *drl* expression is excluded from meristems, but *drl* transcripts accumulate in lateral organs that initiate from meristems, including FM-derived carpel primordia (Fig. 3). Our findings using genetic interaction (Fig. 4A-E), GRN inference (Fig. 4H,I) and expression (Fig. 4J) analyses suggest that DRL1 and ZAG1 may auto-regulate and regulate each other, and potentially converge on a common set of downstream genes to control FM determinacy. We envision a scenario during floret development whereby DRL1 and ZAG1 are initially expressed independent of each other. Later, when their expression domains overlap, auto- and cross-regulation of each factor's expression is maintained and amplified; ultimately, DRL1 and ZAG1 synergistically regulate the expression of downstream genes (Fig. 4K).

Our results suggest that the *drl* genes interact differentially with the distinct developmental potentials of staminate UFMs, LFMs and pistillate UFMs (Figs 1 and 2). UFs and LFs differentially express key regulators (Cacharrón et al., 1999; Skibbe et al., 2008), potentiate differential effects of developmental regulators (Thompson et al., 2009), and derive from slightly different developmental trajectories of the SM (Irish, 1998). Perhaps akin to maize CLAVATA3/ESR-related (CLE) signaling peptides and the *Zm*FON2-LIKE CLE PROTEIN1 (FCP1)-FASCIATED EAR3 (FEA3) primordia-to-meristem feedback circuit (Je et al., 2016), a feedback signaling system from SM- and FM-derived lateral primordia involving the *drl* gene products could provide vital control of stem cell proliferation by integrating hormonal or metabolic cues from incipient and emerging primordia. With some 48 *CLE* genes currently reported in maize (Goad et al., 2017), it is tempting to speculate that differential interactions and/or regulation between *drl*, *zag1* and *CLE* genes and/or gene products could provide non-cell-autonomous control of FM activity from lateral floral primordia. In support of this hypothesis, we found that DRL1 and ZAG1 are predicted to target the genes *fcp1* and *cle35-cle37* (Fig. 4I). Understanding the genetic relationship between CLE-encoding genes and the *drl* and *zag1* genes in maize may contribute further to our understanding of factors that regulate FM activity.

MATERIALS AND METHODS

Genetic stocks and plant growth

Maize plants were grown in the field or the greenhouse. The *drl1* and *drl2* alleles used in this study were described previously (Strable et al., 2017). *drl* alleles were backcrossed to A619, B73, Mo17 and W22 inbred lines at least four times. The effects of *drl1* alleles on floral development were fully penetrant in all backgrounds; backcrosses and F2 introgressions into B73 were used for analyses reported here. The *ifa1* (B73, backcrossed four generations) allele was obtained from Sarah Hake (UC-Berkeley, CA, USA). The *zag1-mum1* (B73, backcrossed many generations) allele was obtained from David Jackson (Cold Spring Harbor Laboratory, NY, USA) and *na1-R* (B73) was obtained from Phillip Becraft (Iowa State University, IA, USA). For quantitative phenotyping, sample sizes per genotype are indicated throughout the manuscript, along with mean±s.e.m. presented with significance calculated using two-tailed Student's *t*-tests. All experiments were performed with two or three independent biological replicates.

Genetic interaction analysis

Allele tests and higher-order mutants were generated using the *drl1-R*, *ifa1* and *drl2-M* alleles and the *zag1-mum1* and *na1-R* alleles. The F_1 progeny from these crosses were grown to maturity and, in the case of triple mutant analysis, self-pollinated. The F_2 progeny were grown to maturity and screened for the *drl1-R* and *drl2-M* alleles (Strable et al., 2017) or for the *zag1-mum1* allele by genotype (9242: AGAGAAGCCAACGCCAWCG-CCTCYATTTCGTC; zag1_F2: GGAATCTGCTAGGCTGAGGC; and zag1_R2: GGTCGTTGAAGTCTTTCCGG). Genotyping primers and assays for *ifa1*, *drl1-R* and *drl2-M*, as well as DNA isolation and PCR conditions were described previously (Strable et al., 2017). Higher-order mutants between *drl1-R*, *drl2-M* and *na1-R* were screened by phenotyping.

Histology

Toluidine Blue O (TBO) (Sigma) staining was performed on mature spikelets. Briefly, TBO was dissolved in 1% sodium borate (w/v) to make a 1% stock solution (w/v). A 0.5% TBO staining solution was made immediately before use by diluting the stock solution with 1% sodium borate. Microtome sections of 10 µm, adhered to a microscope slide, were deparaffinized in Histo-Clear (National Diagnostics) (twice, 10 min each). Slides were passed through a graded ethanol series toward hydration, 1 min each (100%, 100%, 95%, 95%, 70%, 50%, distilled water) and stained in 0.5% TBO staining solution for 3 min. Slides were then passed through a graded series toward dehydration, 30 s each (50%, 70%, 95%, 95%, 100%,

Development (2019) 146, dev171181. doi:10.1242/dev.171181

100%) and Histo-Clear (three times, 5 min each). Slides were coverslip mounted with Permount (Fisher).

Scanning electron microscopy

Field-grown ears 10 mm in length were fixed with 2% paraformaldehyde and 2% glutaraldehyde in cacodylate buffer (0.1 M) at pH 7.2 for at least 24 h at 4°C. After fixation, samples were rinsed three times (15 min each) in cacodylate buffer (0.1 M). Samples were then post-fixed in 1% osmium tetroxide in cacodylate buffer (0.1 M) for 1 h. After several washes with deionized water, samples were dehydrated through a graded ethanol series (25%, 50%, 70%, 85%, 95%, 100%), two changes each for 15 min. Samples were critical point dried using a Denton Vacuum Drying Apparatus, Model DCP-1. Dried materials were mounted on aluminium stubs with double-sided tape and colloidal silver paint and sputter coated with gold-palladium with a Denton Desk II Sputter Coater. Images were captured using a JEOL JSM-5800LV scanning electron microscope at 10 kV (Japan Electronic Optics Laboratory).

RNA *in situ* hybridization and expression analysis

Field-grown 10 mm maize ears were fixed overnight at 4°C in formalin–acetic acid–alcohol (FAA). Samples were dehydrated through a graded ethanol series (50%, 70%, 85%, 95%, 100%) each 1 h, with two changes in 100% ethanol. Samples were then passed through a graded Histo-Clear (National Diagnostics) series (3:1, 1:1, 1:3; ethanol: Histo-Clear) with three changes in 100% Histo-Clear; all changes were 1 h each. Samples were then embedded in Paraplast Plus (McCormick Scientific), sectioned, and hybridized as described previously (Strable et al., 2017). Hybridizations were performed using antisense digoxygenin-labeled RNA probes: *drl1* (Strable et al., 2017), *drl2* (Strable et al., 2017), *kn1* (Jackson et al., 1994), *si1* (Bartlett et al., 2015), *zag1* (Bartlett et al., 2015) and *zyb15/yab8* (JS137-CGATCTCTA-CGCCGCAGC and JS138-GCAGACATACGCAAACATGGG).

Field-grown maize ears less than 8 mm long were dissected away from husk and prophyll primordia and placed individually in 100 µl Trizol (Thermo-Fisher) and stored at −80°C in a 1.5 ml Eppendorf tube until processing. To process, 400 µl Trizol was added and ear tissue was thawed and ground in the presence of Trizol using a plastic drill mount pestle. Total RNA was extracted as per the Trizol manufacturer and treated with RQ1 DNase (Promega) following the protocol outlined by the manufacturer, and converted to cDNA using RNA to cDNA EcoDry Premix (Double Primed) reagents (Takara Bio USA). The cDNA was diluted 1:1 with water, and 1.0 µl was used for PCR. Queried genes and primers used were: *zag1* (zag1_F1 AGACAGCGAACATGATGGGG and zag1_R1 GACATAGTTGGTGCC-AAGCC), *si1* (si1_F1 CGAGGCGTACAAGAACCTGC and si1_R1 CAGTACCTCGGTTGCATTGC) and *ubi1* (ubi_F1 TAAGCTGCCGATG-TGCCTGCGTCG and ubi_R1 CTGAAAGACAGAACATAATGAGCAC-AGGC). PCR followed standard conditions using GoTaq Green Master Mix (Promega Corporation), Ta=58°C, 1 min. extension at 72°C for 33 cycles.

Gene regulatory network inference

Publicly available transcriptome and proteome datasets that represent an atlas of tissues and developmental stages (Walley et al., 2016) were utilized to understand mRNA, non-modified protein and phosphoprotein quantities for *drl1*, *drl2* and *zag1* genes. Transcript abundance [in fragments per kilobase of transcript per million mapped reads (FPKM)], non-modified protein [in distributed normalized spectral abundance factor (dNSAF)] and phosphoprotein (in spectral counts) levels were retrieved directly from this public resource (Walley et al., 2016). We mined each of the seven gene regulatory networks that were generated and reported by Walley and co-workers (2016; Table S10) for regulator-target predictions by classifying DRL1 or ZAG1 as TF regulators and retrieving the set inferred regulator-target mRNA pairs with high-confidence edge scores. We report on high-confidence predicted target mRNAs in the *YABBY*, *MADS-box* and *CLE* gene families as well as other maize floral-expressed genes.

Accession numbers

Genes referred to in this study include: *drl1*, GRMZM2G088309; *drl2*, GRMZM2G102218; *kn1*, GRMZM2G017087; *si1*, GRMZM2G139073; *ubi1*, GRMZM2G409726; *zag1*, GRMZM2G052890; *zyb15/yab8*, GRMZM2G529859.

Acknowledgements

We thank Harry Horner and Tracey Stewart at the Iowa State University Bessey Microscopy Facility for assistance with scanning electron microscopy and Pete Lelonek for plant care. Many thanks to Clint Whipple for generously sharing the si1 probe for RNA in situ hybridization and to Beth Thompson for discussions on *ifa1*. We thank Justin Walley for helpful discussions on incorporating GRN analysis. We are grateful for the many former undergraduate students, especially Sarah Briggs, Emery Peyton and Charlie Beeler, for their help in our summer genetics nurseries. Many thanks to Erin Irish and Erica Unger-Wallace for insightful discussions and comments on the manuscript. We also appreciate helpful suggestions and comments from three anonymous reviewers.

Competing interests

The authors declare no competing or financial interests.

Author contributions

Conceptualization: J.S.; Methodology: J.S.; Validation: J.S.; Formal analysis: J.S, E.V..; Investigation: J.S.; Resources: E.V.; Writing - original draft: J.S.; Writing - review & editing: J.S., E.V.; Visualization: J.S.; Supervision: E.V.; Project administration: J.S., E.V.; Funding acquisition: E.V.

Funding

This work was supported by the National Science Foundation (IOS-1238202).

Supplementary information

Supplementary information available online at
http://dev.biologists.org/lookup/doi/10.1242/dev.171181.supplemental

References

Alvarez, J. and Smyth, D. R. (1999). *CRABS CLAW* and *SPATULA*, two *Arabidopsis* genes that control carpel development in parallel with *AGAMOUS*. *Development* **126**, 2377-2386.

Ambrose, B. A., Lerner, D. R., Ciceri, P., Padilla, C. M., Yanofsky, M. F. and Schmidt, R. J. (2000). Molecular and genetic analyses of the silky1 gene reveal conservation in floral organ specification between Eudicots and Monocots. *Mol. Cell* **5**, 569-579.

Bartlett, M. E., Williams, S. K., Taylor, Z., DeBlasio, S., Goldshmidt, A., Hall, D. H., Schmidt, R. J., Jackson, D. P. and Whipple, C. J. (2015). The maize *PI/GLO* ortholog *Zmm16/sterile tassel silky ear1* interacts with the zygomorphy and sex determination pathways in flower development. *Plant Cell* **27**, 3081-3098.

Becraft, P. W. and Freeling, M. (1994). Genetic analysis of *Rough sheath1* developmental mutants of maize. *Genetics* **136**, 295-311.

Bensen, R. J., Johal, G. S., Crane, V. C., Tossberg, J. T., Schnable, P. S., Meeley, R. B. and Briggs, S. P. (1995). Cloning and characterization of the maize *An1* gene. *Plant Cell* **7**, 75-84.

Bonnett, O. T. (1953). Developmental morphology of the vegetative and floral shoots of maize. *Ann. Mo. Bot. Gard.* **35**, 269-287.

Bowman, J. L. and Smyth, D. R. (1999). *CRABS CLAW*, a gene that regulates carpel and nectary development in *Arabidopsis*, encodes a novel protein with zinc finger and helix-loop-helix domains. *Development* **126**, 2387-2396.

Cacharrón, J., Saedler, H. and Theißen, G. (1999). Expression of MADS box genes *ZMM8* and *ZMM14* during inflorescence development of *Zea mays* discriminates between the upper and the lower floret of each spikelet. *Dev. Genes Evol.* **209**, 411-420.

Cheng, P. C., Greyson, R. I. and Walden, D. B. (1983). Organ initiation and the development of unisexual flowers in the tassel and ear of *Zea mays*. *Am. J. Bot.* **70**, 450-462.

Chuck, G., Meeley, R. and Hake, S. (2008). Floral meristem initiation and meristem cell fate are regulated by the maize *AP2* genes *ids1* and *sid1*. *Development* **135**, 3013-3019.

Clifford, H. T. (1987). Spikelet and floral morphology. In *Grass Systematics and Evolution* (ed. T. R. Soderstrom, K. W. Hilu, C. S. Campbell and M. E. Barkworth), pp. 21-30. Washington, DC: Smithsonian Institution Press.

Coen, E. S. and Meyerowitz, E. M. (1991). The war of the whorls: genetic interactions controlling flower development. *Nature* **353**, 31-37.

Dreni, L., Pilatone, A., Yun, D., Erreni, S., Pajoro, A., Caporali, E., Zhang, D. and Kater, M. M. (2011). Functional analysis of all AGAMOUS subfamily members in rice reveals their roles in reproductive organ identity determination and meristem determinacy. *Plant Cell* **23**, 2850-2863.

Eshed, Y., Baum, S. F. and Bowman, J. L. (1999). Distinct mechanisms promote polarity establishment in carpels of Arabidopsis. *Cell* **99**, 199-209.

Evans, M. M. S. (2007). The *indeterminate gametophyte1* gene of maize encodes a LOB domain protein required for embryo sac and leaf development. *Plant Cell* **19**, 46-62.

Fourquin, C., Vinauger-Douard, M., Fogliani, B., Dumas, C. and Scutt, C. P. (2005). Evidence that crabs claw and tousled have conserved their roles in carpel development since the ancestor of the extant angiosperms. *Proc. Natl. Acad. Sci. USA* **102**, 4649-4654.

Fourquin, C., Primo, A., Martínez-Fernández, I., Huet-Trujillo, E. and Ferrándiz, C. (2014). The *CRC* orthologue from *Pisum sativum* shows conserved functions in carpel morphogenesis and vascular development. *Ann. Bot.* **114**, 1535-1544.

Gallavotti, A., Malcomber, S., Gaines, C., Stanfield, S., Whipple, C., Kellogg, E. and Schmidt, R. J. (2011). BARREN STALK FASTIGIATE1 is an AT-Hook protein required for the formation of maize ears. *Plant Cell* **23**, 1756-1771.

Goad, D. M., Zhu, C. and Kellogg, E. A. (2017). Comprehensive identification and clustering of CLV3/ESR-related (CLE) genes in plants finds groups with potentially shared function. *New Phytol.* **216**, 605-616.

Goldshmidt, A., Alvarez, J. P., Bowman, J. L. and Eshed, Y. (2008). Signals derived from *YABBY* gene activities in organ primordia regulate growth and partitioning of *Arabidopsis* shoot apical meristems. *Plant Cell* **20**, 1217-1230.

Gómez-Mena, C., de Folter, S., Costa, M. M., Angenent, G. C. and Sablowski, R. (2005). Transcriptional program controlled by the floral homeotic gene AGAMOUS during early organogenesis. *Development* **132**, 429-438.

Greb, T. and Lohmann, J. U. (2016). Plant stem cells. *Curr. Biol.* **26**, R816-R821.

Hartwig, T., Chuck, G. S., Fujioka, S., Klempien, A., Weizbauer, R., Potluri, D. P. V., Choe, S., Johal, G. S. and Schulz, B. (2011). Brassinosteroid control of sex determination in maize. *Proc. Natl. Acad. Sci. USA* **108**, 19814-19819.

Irish, E. E. (1997). Class II tassel seed mutations provide evidence for multiple types of inflorescence meristems in maize (Poaceae). *Am. J. Bot.* **84**, 1502-1515.

Irish, E. E. (1998). Grass spikelets: a thorny problem. *BioEssays* **20**, 789-793.

Irish, E. E., Szymkowiak, E. J. and Garrels, K. (2003). The *wandering carpel* mutation of *Zea mays* (Gramineae) causes misorientation and loss of zygomorphy in flowers and two-seeded kernels. *Am. J. Bot.* **90**, 551-560.

Jackson, D., Veit, B. and Hake, S. (1994). Expression of maize KNOTTED1 related homeobox genes in the shoot apical mersitem predicts patterns of morphogenesis in the vegetative shoot. *Development* **120**, 405-413.

Je, B. I., Gruel, J., Lee, Y. K., Bommert, P., Arevalo, E. D., Eveland, A. L., Wu, Q., Goldshmidt, A., Meeley, R., Bartlett, M. et al. (2016). Signaling from maize organ primordia via FASCIATED EAR3 regulates stem cell proliferation and yield traits. *Nat. Genet.* **48**, 785-791.

Juarez, M. T., Twigg, R. W. and Timmermans, M. C. P. (2004). Specification of adaxial cell fate during maize leaf development. *Development* **131**, 4533-4544.

Kiesselbach, T. (1949). *The Structure and Reproduction of Corn*. Lincoln, NE: Univeristy of Nebraska College of Agriculture.

Laudencia-Chingcuanco, D. and Hake, S. (2002). The *indeterminate floral apex1* gene regulates meristem determinacy and identity in the maize inflorescence. *Development* **129**, 2629-2638.

Lenhard, M., Bohnert, A., Jürgens, G. and Laux, T. (2001). Termination of stem cell maintenance in Arabidopsis floral meristems by interactions between *WUSCHEL* and *AGAMOUS*. *Cell* **105**, 805-814.

Li, H., Liang, W., Hu, Y., Zhu, L., Yin, C., Xu, J., Dreni, L., Kater, M. M. and Zhang, D. (2011). Rice *MADS6* interacts with the floral homeotic genes *SUPERWOMAN1, MADS3, MADS58, MADS13,* and *DROOPING LEAF* in specifying floral organ identities and meristem fate. *Plant Cell* **23**, 2536-2552.

Lohmann, J. U., Hong, R. L., Hobe, M., Busch, M. A., Parcy, F., Simon, R. and Weigel, D. (2001). A molecular link between stem cell regulation and floral patterning in *Arabidopsis*. *Cell* **105**, 793-803.

Mena, M., Ambrose, B. A., Meeley, R. B., Briggs, S. P., Yanofsky, M. F. and Schmidt, R. J. (1996). Diversification of C-function activity in maize flower development. *Science* **274**, 1537-1540.

Nakayama, H., Yamaguchi, T. and Tsukaya, H. (2010). Expression patterns of *AaDL*, a *CRABS CLAW* ortholog in *Asparagus asparagoides* (Asparagaceae), demonstrate a stepwise evolution of *CRC*/*DL* subfamily of *YABBY* genes. *Am. J. Bot.* **97**, 591-600.

Ó'Maoiléidigh, D. S., Wuest, S. E., Rae, L., Raganelli, A., Ryan, P. T., Kwaśniewska, K., Das, P., Lohan, A. J., Loftus, B., Graciet, E. et al. (2013). Control of reproductive floral organ identity specification in Arabidopsis by the C function regulator AGAMOUS. *Plant Cell* **25**, 2482-2503.

Ó'Maoiléidigh, D. S., Stewart, D., Zheng, B., Coupland, G. and Wellmer, F. (2018). Floral homeotic proteins modulate the genetic programs for leaf development to suppress trichome formation in flowers. *Development* **145**, dev157784.

Orashakova, S., Lange, M., Lange, S., Wege, S. and Becker, A. (2009). The CRABS CLAW ortholog from California poppy (*Eschscholzia californica*, Papaveraceae), EcCRC, is involved in floral meristem termination, gynoecium differentiation and ovule initiation. *Plant J.* **58**, 682-693.

Payne, T., Johnson, S. D. and Koltunow, A. W. (2004). KNUCKLES (KNU) encodes a C2H2 zinc-finger protein that regulates development of basal pattern elements of the Arabidopsis gynoecium. *Development* **131**, 3737-3749.

Pelaz, S., Ditta, G. S., Baumann, E., Wisman, E. and Yanofsky, M. F. (2000). B and C floral organ identity functions require *SEPALLATA* MADS-box genes. *Nature* **405**, 200-203.

Pfannebecker, K. C., Lange, M., Rupp, O. and Becker, A. (2017). Seed plant-specific gene lineages involved in carpel development. *Mol. Biol. Evol.* **34**, 925-942.

Randolph, F. R. (1926). Memoir 102: A cytological study of two types of variegated pericarp in maize. Ithaca, NY; Cornell University, Agricultural Experiment Station.

Schmidt, R. J., Veit, B., Mandel, M. A., Mena, M., Hake, S. and Yanofsky, M. F. (1993). Identification and molecular characterization of *ZAG1*, the maize homolog of the Arabidopsis floral homeotic gene *AGAMOUS*. *Plant Cell* **5**, 729-737.

Skibbe, D. S., Wang, X., Borsuk, L. A., Ashlock, D. A., Nettleton, D. and Schnable, P. S. (2008). Floret-specific differences in gene expression and support for the hypothesis that tapetal degeneration of *Zea mays* L. occurs via programmed cell death. *J. Genet. Genomics* **35**, 603-616.

Strable, J., Wallace, J. G., Unger-Wallace, E., Briggs, S., Bradbury, P. J., Buckler, E. S. and Vollbrecht, E. (2017). Maize *YABBY* genes *drooping leaf1* and *drooping leaf2* affect agronomic traits by regulating leaf architecture. *Plant Cell* **29**, 1622-1641.

Sun, B., Xu, Y., Ng, K.-H. and Ito, T. (2009). A timing mechanism for stem cell maintenance and differentiation in the Arabidopsis floral meristem. *Genes Dev.* **23**, 1791-1804.

Sun, B., Looi, L.-S., Guo, S., He, Z., Gan, E.-S., Huang, J., Xu, Y., Wee, W.-Y. and Ito, T. (2014). Timing mechanism dependent on cell division is invoked by Polycomb eviction in plant stem cells. *Science* **343**, 1248559.

Thompson, B. E., Bartling, L., Whipple, C., Hall, D. H., Sakai, H., Schmidt, R. and Hake, S. (2009). *bearded-ear* encodes a MADS box transcription factor critical for maize floral development. *Plant Cell* **21**, 2578-2590.

Walley, J. W., Sartor, R. C., Shen, Z., Schmitz, R. J., Wu, K. J., Urich, M. A., Nery, J. R., Smith, L. G., Schnable, J. C., Ecker, J. R. et al. (2016). Integration of omic networks in a developmental atlas of maize. *Science* **353**, 814-818.

Wang, H., Nussbaum-Wagler, T., Li, B., Zhao, Q., Vigouroux, Y., Faller, M., Bomblies, K., Lukens, L. and Doebley, J. F. (2005). The origin of the naked grains of maize. *Nature* **436**, 714-719.

Whipple, C. J., Hall, D. H., DeBlasio, S., Taguchi-Shiobara, F., Schmidt, R. J. and Jackson, D. P. (2010). A conserved mechanism of bract suppression in the grass family. *Plant Cell* **22**, 565-578.

Whipple, C. J., Kebrom, T. H., Weber, A. L., Yang, F., Hall, D., Meeley, R., Schmidt, R., Doebley, J., Brutnell, T. P. and Jackson, D. P. (2011). *grassy tillers1* promotes apical dominance in maize and responds to shade signals in the grasses. *Proc. Natl. Acad. Sci. USA* **108**, E506-E512.

Yamada, T., Yokota, S., Hirayama, Y., Imaichi, R., Kato, M. and Gasser, C. S. (2011). Ancestral expression patterns and evolutionary diversification of YABBY genes in angiosperms. *Plant J.* **67**, 26-36.

Yamaguchi, T., Nagasawa, N., Kawasaki, S., Matsuoka, M., Nagato, Y. and Hirano, H.-Y. (2004). The YABBY gene *DROOPING LEAF* regulates carpel specification and midrib development in *Oryza sativa*. *Plant Cell* **16**, 500-509.

Yamaguchi, T., Lee, Y. D., Miyao, A., Hirochika, H., An, G. and Hirano, H.-Y. (2006). Functional diversification of the two C-class MADS box genes *OSMADS3* and *OSMADS58* in *Oryza sativa*. *Plant Cell* **18**, 15-28.

Yamaguchi, N., Huang, J., Xu, Y., Tanoi, K. and Ito, T. (2017). Fine-tuning of auxin homeostasis governs the transition from floral stem cell maintenance to gynoecium formation. *Nat. Commun.* **8**, 1125.

Yamaguchi, N., Huang, J., Tatsumi, Y., Abe, M., Sugano, S. S., Kojima, M., Takebayashi, Y., Kiba, T., Yokoyama, R., Nishitani, K. et al. (2018). Chromatin-mediated feed-forward auxin biosynthesis in floral meristem determinacy. *Nat. Commun.* **9**, 5290.

Yanofsky, M. F., Ma, H., Bowman, J. L., Drews, G. N., Feldmann, K. A. and Meyerowitz, E. M. (1990). The protein encoded by the *Arabidopsis* homeotic gene *agamous* resembles transcription factors. *Nature* **346**, 35-39.

SUPPLEMENTARY INFORMATION

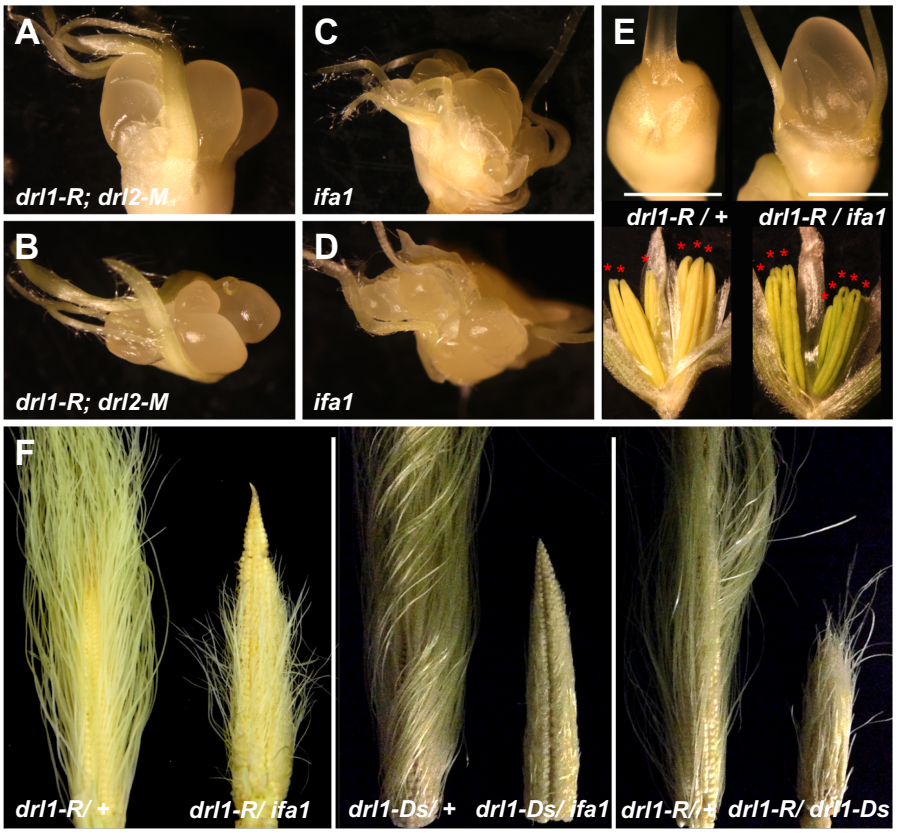

Figure S1. Complementation tests for *drl1* alleles. (**A-D**) Dissected pistillate florets showing multiple nucelli in *drl1-R; drl2-M* (**A,B**) and in *drl1-ifa1* (**C,D**). (**E**) Dissected pistillate and staminate florets of F_1 progeny of *drl1-R/+* heterozygous and *drl1-R/ifa1* trans-heterozygous siblings. (**F**) Mature ears of *drl1-R/+* sibling and *drl1-R/ifa1* (left panel); *drl1-Ds/+* sibling and *drl1-Ds/ifa1* (middle panel); and *drl1-R/+* sibling and *drl1-R/drl1-Ds* (right panel). Asterisks mark mature anthers. Scale bar: 2 mm.

Figure S2. Mature ear and floret of *drl1-R; drl2-DsD08*. Mature ears of normal sibling and *drl1-R; drl2-DsD08* in the W22 (non-enhancing) inbred background. Inset, dissected *drl1-R; drl2-DsD08* floret showing multiple nucelli.

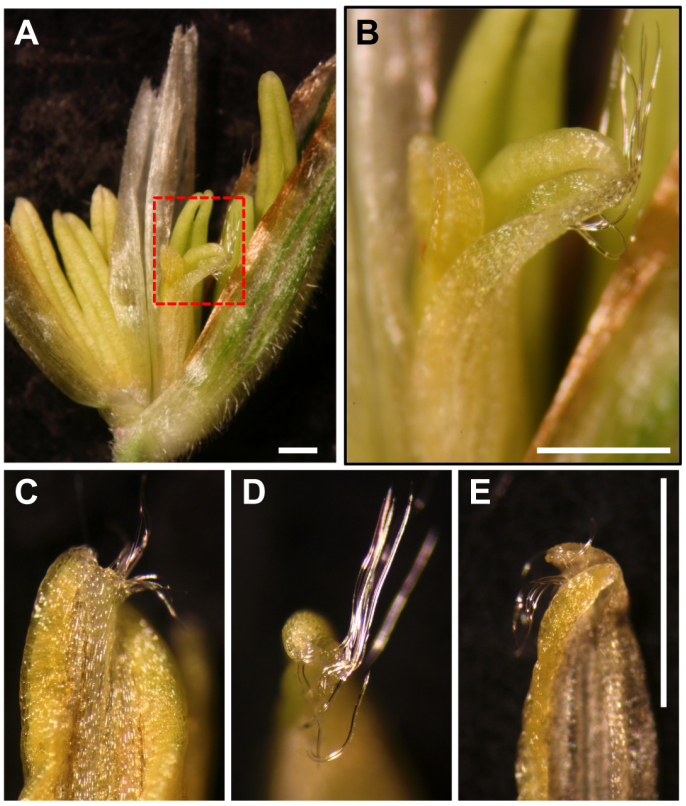

Figure S3. Macrohairs on *drl1; drl2* ectopic anthers. (**A**) Dissected staminate floret with ectopic stamen. (**B**) Boxed area in (**A**) enlarged to show macrohairs along the apical ridge of the anther. (**C-E**) Anthers of ectopic stamens are often amorphic showing deformed theca and empty pollen sacs in addition to macrohairs. Scale bars: 1 mm.

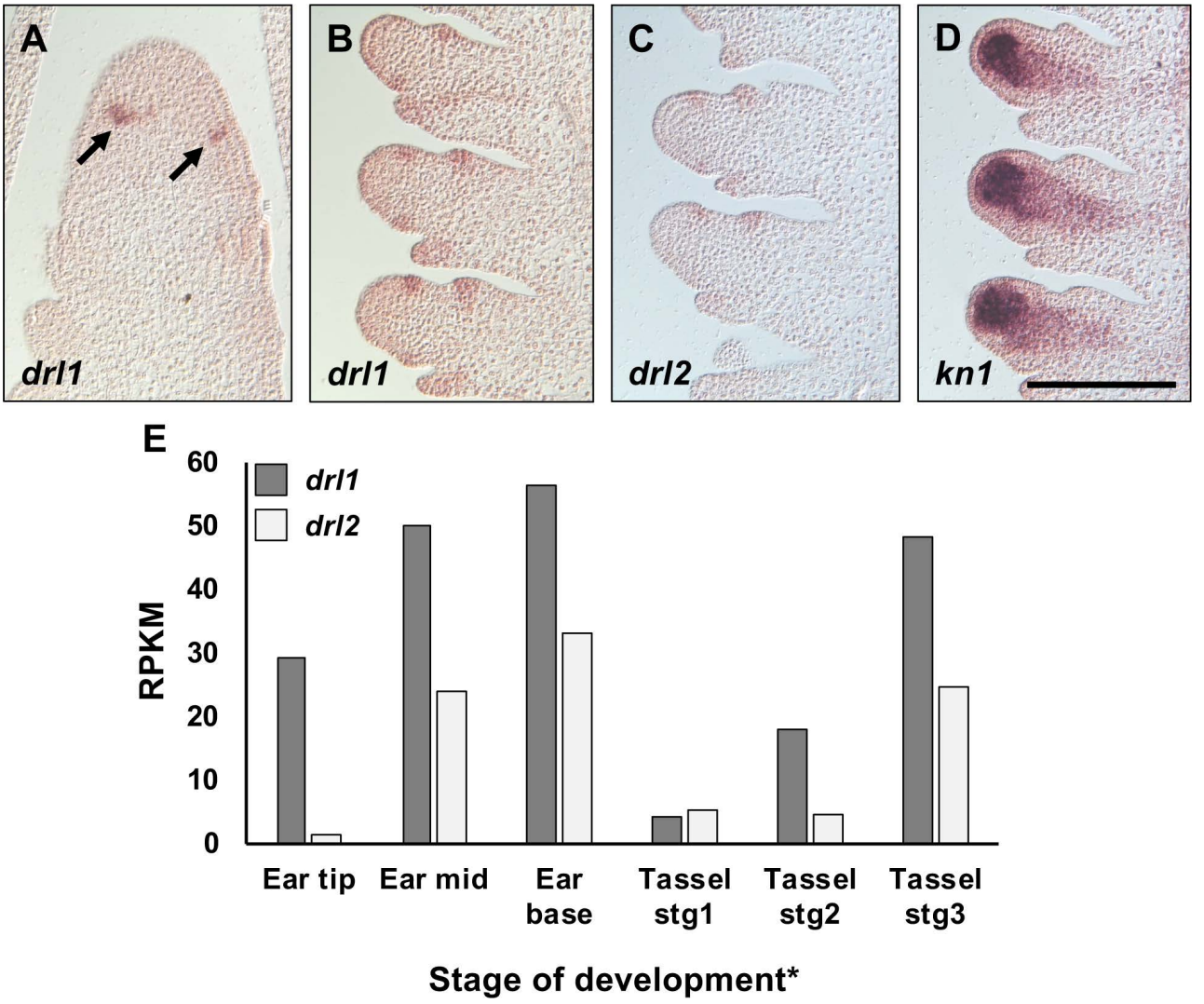

Figure S4. Expression of *drl* genes throughout inflorescence development. (**A**) Longitudinal section through IM of a developing ear hybridized with antisense RNA probes to *drl1*; arrow points to *drl1* transcript accumulation in presumptive cryptic bract anlagen. (**B,C**) Longitudinal sections through early-stage B73 pistillate florets hybridized with antisense RNA probes to *drl1* (**B,** shorter exposer cf. Fig. 3C), *drl2* (**C**) or *kn1* (**D**); Scale bar: 200 µm. (**E**) Publicly-available RNAseq data (www.maizeinflorescence.org) across B73 developing inflorescences filtered for relative transcript accumulation for *drl1* and *drl2* genes. Ear tip, 1 mm section from the tip of a 10 mm ear (enriched for IM and SPMs); Ear mid, 2 mm section 2 mm from the tip of a 10 mm ear (enriched for SMs); Ear base, 2 mm section 6 mm from the tip of a 10 mm ear (enriched for FMs); Tassel stg1, 1-2 mm; Tassel stg2, 3-4 mm; Tassel stg3, 5-7mm.

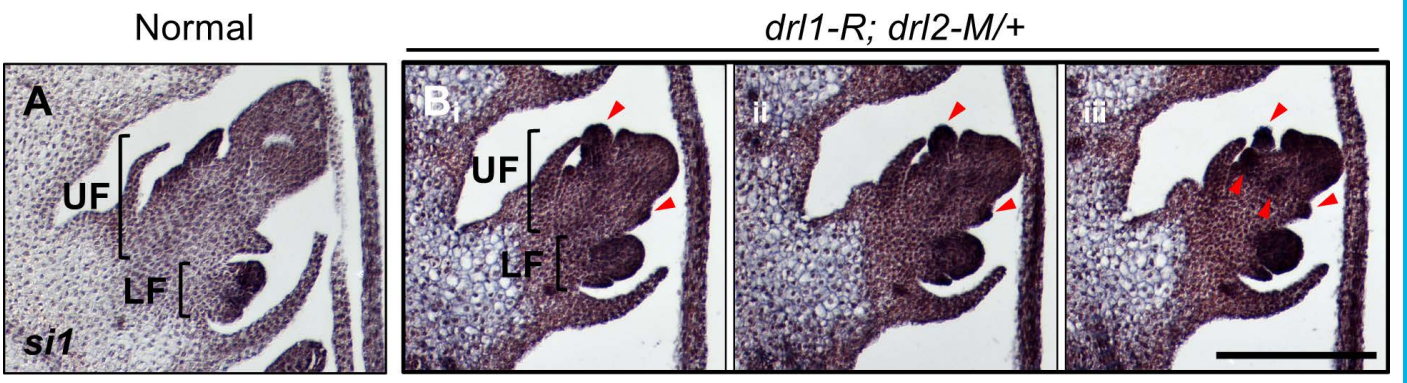

Figure S5. RNA *in situ* hybridization of *si1* in late-stage normal and *drl1-R; drl2-M/+* pistillate florets. Longitudinal section through late-stage pistillate florets from normal (**A**) and *drl1-R; drl2-M/+* (**B**) ears hybridized with an antisense RNA probe to *si1*. $B_{i\text{-}iii}$ represent serial sections. Arrowheads point to ectopic accumulation of *si1* transcripts in putative lodicule-like or stamen-like primordia. Scale bar: 200 µm.

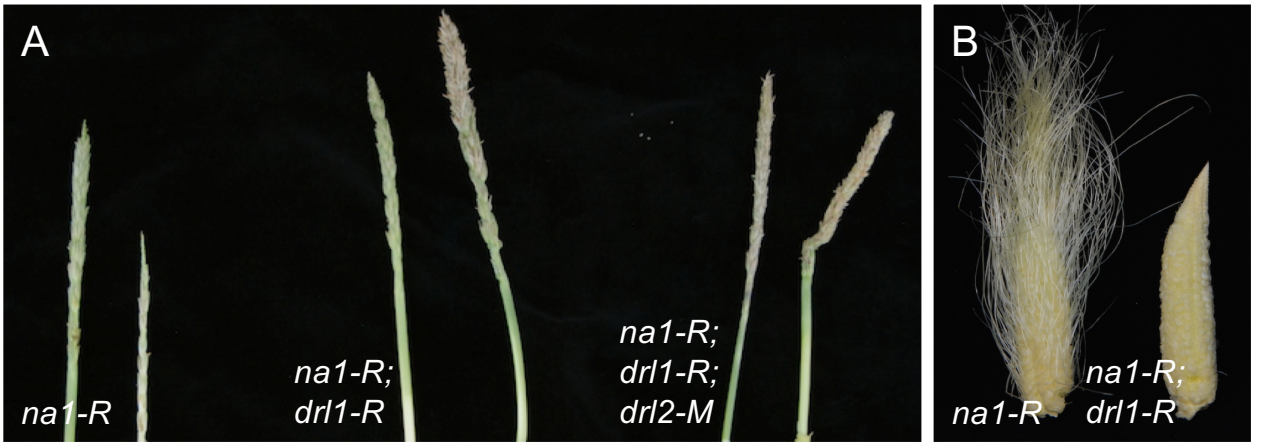

Figure S6. Genetic interaction analysis of na1-R, drl1-R and drl2-M mutants. (**A**) Unbranched tassels from field-grown plants showing normal, staminate florets. (**B**) Ears from field-grown plants. Field-grown *na1-R; drl1-R; drl2-M* triple mutants were earless.